PAN
ARCHIVES OF ACOUSTICS
Vol. **45**, No. 2, pp. 209–219 (2020)
DOI: 10.24425/aoa.2020.132495

Research Paper

Direction Estimation and Tracking of Coherent Sources Using a Single Acoustic Vector Sensor

Mohd WAJID[(1),(2)*], Arun KUMAR[(1)], Rajendar BAHL[(1)]

[(1)] *Centre for Applied Research in Electronics*
Indian Institute of Technology Delhi
New Delhi, India
e-mail: {arunkm, rbahl}@care.iitd.ac.in

[(2)] *Department of Electronics Engineering, Z.H.C.E.T.*
Aligarh Muslim Univesity
Aligarh, India
*Corresponding Author e-mail: wajidiitd@ieee.org

(*received June 12, 2019; accepted February 18, 2020*)

A single acoustic vector sensor (AVS) cannot be used to find the direction-of-arrival (DOA) of two or more coherent (fully correlated) sources. We have proposed a technique for estimating DOAs (in 2D geometry) of two simultaneous coherent sources using single AVS under the assumption that acoustic sources enter in the field sequentially. The DOA estimation has been investigated with two different configurations of AVS, each consisting of three microphones in a plane. The technique has been also applied in tracking (a) an acoustic source in the presence of stationary interfering coherent source and (b) two coherent sources when the sources are changing their locations alternatively. The experimental environment has been generated using the Finite-Element Method tool viz. COMSOL to corroborate the proposed scheme.

Keywords: acoustic intensity; acoustic vector sensor; Direction of Arrival (DOA); Finite Element Method (FEM); tracking of acoustic source.

1. Introduction

Acoustic vector sensor (AVS) is a device that measures pressure and particle velocity at a single point in space. The pressure and particle velocity determine the acoustic intensity produced by an acoustic source. The acoustic intensity is a vector quantity, whose direction is from an acoustically radiating source to the AVS. In the free field, the direction of arrival of an acoustic source can be estimated by means of acoustic intensity using a single AVS (Cao *et al.*, 2016; de Bree, 2003; Hawkes, Nehorai, 1998; Lockwood, Jones, 2006; Nehorai, Paldi, 1994). In recent years, researchers have focused on AVS based intensity measurement and its use in direction of arrival estimation of sound sources (Kotus, 2012; 2015; Kotus, Czyżewski, 2010; Kotus *et al.*, 2014; 2016; Kotus, Kostek, 2015; Odya *et al.*, 2017; Wajid *et al.*, 2017a; 2017b). As the intensity-based DOA estimation does not need any search in the space, therefore it is suitable for real-time applications. However, acoustic intensity-based DOA estimation of multiple coherent sources using a single acoustic vector sensor is a non-viable task. This is due to the fact that, if two or more acoustic sources are present in the field, then the estimated intensity vector will be the weighted sum of the true intensity vectors caused by each source. These weights are a function of energy and frequency of the source signals (Wajid *et al.*, 2017c). In this paper, a real-time DOA estimation of two coherent (fully correlated) sources using a single AVS has been proposed. We have studied the DOA estimation performance of simultaneous coherent acoustic sources using two different AVS configurations viz. L-shaped AVS (LAVS) and triangular-shaped AVS (TAVS). Each of these AVS is consist of three omnidirectional microphones (or hydrophones) only.

A subspace technique like MUltiple SIgnal Classification (MUSIC) based on the covariance matrix of the particle velocity signals also fails in multiple coher-

ent source localization. These subspace techniques are high-resolution methods for DOA estimation, however, they can be applied only for uncorrelated or partially correlated sources (Chen, Zhao, 2015; Dmochowski *et al.*, 2007; Palanisamy *et al.*, 2012; Qian *et al.*, 2014; Ran, Zhang, 2004). In multipath propagation environments, the received signal from multiple directions is coherent with the direct path signal. This will cause a rank deficiency in the covariance matrix of the received signal vector and hence the noise subspace cannot be identified, thereby, leading to false estimation of DOAs. So finding DOA of multiple coherent sources with a single vector sensor is a challenging task.

There are microphone-array based solutions available for the localization of coherent sources (Du, Kirlin, 1991; Evans *et al.*, 1982; Han, Zhang, 2005; Pillai, Kwon, 1989; Qian *et al.*, 2014; Shan *et al.*, 1985). The spatial smoothing technique (Du, Kirlin, 1991; Evans *et al.*, 1982; Shan *et al.*, 1985), where the array of microphones is first partitioned into a number of smaller arrays and the average of their covariance matrices is used. However, these techniques cause degradation of DOA resolution due to aperture loss. Also, it is an under-determined approach of DOA estimation, as the only M/2 number of coherent sources can be handled using the M number of sensors in the uniform linear array (ULA). More number of coherent sources i.e. up to 75% of the number of sensors can be resolved if forward/backward spatial smoothing is used (Pillai, Kwon, 1989). Han and Zhang (2005) have used symmetric ULA, where Toeplitz matrices are generated using each row of the covariance matrix, which enables the use of subspace technique for resolving coherent sources. Qian *et al.* (2014) have proposed coherent source DOA estimation which does not require *a priori* knowledge of the number of sources as in subspace technique. It is based on the diagonalization structure of the Toeplitz matrices (as obtained by Han and Zhang (2005)) generated from the rows of covariance matrices, which decorrelate the covariance matrix of the coherent signal. Then a novel spatial spectrum is suggested where a dimensional search is used for DOA estimation. However, it is applied for ULA, and not for an AVS and the source signals are assumed to be of equal power. Also, it requires searching in the space which makes the procedure unsuitable for real-time applications.

Palanisamy *et al.* (2012) and Liu *et al.* (2013) have presented a method for the localization of highly correlated signals using an L-shaped and rectangular-shaped array of AVS respectively. It involves the decorrelation of the coherent signals and the signal subspace has been generated from correlation matrices of sub-arrays. They have used a propagator based technique that does not need any eigen-decomposition or singular-value decomposition as in the Estimation of Signal Parameters via Rotational Invariance Techniques (ESPRIT). Also, it requires only linear operations and does not need any search in the space, hence it requires less computation. However, the technique developed needs an array of AVS and they have used a large number of AVSs i.e. 8, 12, and 16 in their simulation. Also, they have assumed the ideal signal model of the AVS. Chen and Zhao (2005)have proposed a coherent signal-subspace method for wideband source (Wang, Kaveh, 1985) using a linear array of AVS. Also, they have compared the performance for an eight AVS element ULA and 8 pressure sensor ULA for the wideband coherent sources. The AVS ULA allows spatially under-sampled arrays and removes end-fire direction ambiguity. Wu *et al.* (2014) have also proposed a method to localise the closely spaced coherent sources by using a linear array of AVS.

A maximum of two non-coherent sources' DOA can be estimated using a single AVS using a subspace technique (Hochwald, Nehorai, 1996). However, acoustic intensity based DOA estimation is computationally efficient as it does not need to calculate the covariance matrix and search in the space, but it can determine the DOA of a single source. When two coherent sources with different power are present in the field, the estimated intensity points to the direction as a weighted linear combination of the individual intensity vectors (Wajid *et al.*, 2017c). Therefore, DOAs estimation using a single AVS is not viable.

The existing techniques as discussed above, either employ AVS/microphone-array (large aperture) and/or need a search in the space. However, the proposed technique uses single AVS and does not require any search in the space. Therefore, it can be used to find the DOA for real-time applications and suitable for the portable surveillance systems due to its small size. We have remodeled the intensity components where intensity components of a first source will be removed from the intensity components due to two simultaneous sources, and the resulting remodeled intensity can be used for DOA estimation of the second source. There may arise many situations of interest where initially one source is available in the field then another acoustic source emerges. For example, when a torpedo is going to attack a ship belonging to an enemy, the enemy ship may leave a decoy at its position and changes its location to confuse the torpedo. Under such a scenario, the sequential estimation method is preferred. The proposed technique is directly applicable in the estimation of DOA of the enemy ship in the presence of decoy or in the related scenarios due to reverberation. The procedure for DOA estimation of two coherent sources using TAVS and LAVS configurations have been discussed analytically along with FEM simulation validation. The same approach can be applied to any AVS configuration. The continuous tracking of two sequential coherent sources using a single AVS has also been discussed in two different scenarios. First,

when a source is changing its location in the presence of stationary interfering coherent source. Second, when two coherent sources are changing their locations alternatively.

The paper is organized as follows. Section 2 gives the assumptions that are being made while formulating DOA of multiple coherent sources using a single AVS. In Sec. 3, the concept of acoustic intensity based DOA estimation and AVS configurations for DOA estimation are discussed. Section 4 gives the approach of DOA estimation of coherent sources using single AVS. Numerical simulation setup and results for DOA estimation of two simultaneous coherent sources and their tracking are given in Sec. 5. Section 6 concludes the paper.

2. Assumptions

The following assumptions are being made while devising the DOA estimation model of multiple coherent sources using a single acoustic vector sensor:

A1) The medium of propagation of the acoustic waves is quiescent, homogeneous and isotropic.

A2) Far-field is considered i.e., the AVS is receiving a planar acoustic wave (maximum wavelength is at least two times smaller than the source-to-sensor distance).

A3) The acoustic sources are of point size (i.e., the dimension of the acoustic source is much smaller than the source-to-sensor distance).

A4) The microphones are of point size and the AVS dimension is much small than the minimum wavelength.

A5) All microphones are identical and have an omnidirectional beam pattern. The microphones within the AVS configuration does not have any placement inaccuracies.

A6) The additive noise at the microphone is Gaussian with zero mean and its covariance matrix will have zero off-diagonal elements. It is also assumed the source signals and noise are uncorrelated.

A7) The acoustic coherent sources enter the field sequentially. All sources in the field can change their angular location with the assumption that at any one time only one of the sources changes its angular position.

3. Acoustic intensity based DOA estimation and AVS configurations

Acoustic intensity $\mathbf{I}$ is a vector quantity derived from acoustic pressure and particle velocity, given as

$$\mathbf{I}(\mathbf{r},t) = p(\mathbf{r},t)\mathbf{v}(\mathbf{r},t), \tag{1}$$

where p is the pressure, $\mathbf{v}$ is the particle velocity, $\mathbf{r}$ is the position vector of the sensor, and t is the time instant. The DOA $\widehat{\theta}$ of an acoustic source is estimated using the arc-tan method,

$$\widehat{\theta} = \arctan\left(\frac{\widehat{I}_x}{\widehat{I}_y}\right), \tag{2}$$

where $\widehat{I}_x$ and $\widehat{I}_y$ are the estimate of orthogonal components of time-average acoustic intensities along the x-axis and y-axis respectively. The estimated DOA $\widehat{\theta}$ is measured with respect to y-axes in the clockwise direction. The time-average acoustic intensity component along the x-axis is estimated using pressure measurements at two distinct points with a spatial separation of d. The two microphones are kept at coordinates $(0,0)$ and $(d,0)$ which records the signals $p_o(t)$ and $p_h(t)$ respectively. If the minimum wavelength $\lambda_{\min}$ of the acoustic signal is much greater than the microphone separation d i.e. $d \lll \lambda_{\min}$, then the estimated intensity component $\widehat{I}_x$ is given by

$$\widehat{I}_x = -\frac{1}{\rho_o d}\int_0^\infty \frac{1}{\omega}\mathrm{Im}\left[\Gamma_{p_o p_h}(\omega)\right]\mathrm{d}\omega, \tag{3}$$

where ρ_o is the medium density and $\Gamma_{p_o p_h}(\omega)$ is the cross power spectral density (CPSD) between the signals $p_o(t)$ and $p_h(t)$, in the subsequent paper same notation conventions are used for CPSD representation between any two signals. (For more detail and derivation of Eq. (3), see (Chung, 1978; Fahy, 1977; Krishnappa, 1981; Miah, Hixon, 2010; Moschioni *et al.*, 2007; Rinford, 1981; Thompson, Tree, 1981; Wajid *et al.*, 2016a).

Similarly, the time-averaged acoustic intensity component along the y-axis is given by

$$\widehat{I}_y = -\frac{1}{\rho_o d}\int_0^\infty \frac{1}{\omega}\mathrm{Im}\left[\Gamma_{p_o p_v}(\omega)\right]\mathrm{d}\omega, \tag{4}$$

where, $p_v(t)$ is the pressure signal acquired by the microphone located at coordinate $(0,\, d)$.

Figures 1 and 2 show the two AVS configurations, namely, L-shape AVS (LAVS) and triangular

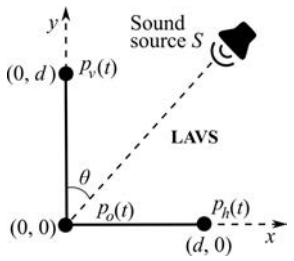

Fig. 1. LAVS constructed using three omnidirectional microphones placed at x-axis, y-axis and origin, and the recorded pressure signals are $p_h(t)$, $p_v(t)$, and $p_o(t)$ respectively (note: dark circles indicate microphone).

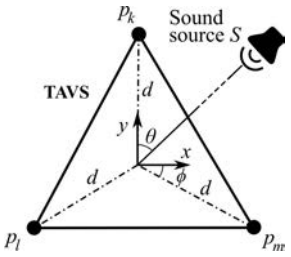

Fig. 2. TAVS constructed using three omnidirectional microphones placed at the three vertices of an equilateral triangle (distance of each microphone from origin is d), and their pressure signals are $p_k(t)$, $p_l(t)$, and $p_m(t)$ (note: dark circles indicate microphone and $\phi = 30^\circ$).

AVS (TAVS) each is constructed using three omnidirectional microphones. The DOA estimation of an acoustic source has been derived for these two AVS configurations.

Let an acoustic source S_1 be present in the field at an angle θ^{S_1}. The signal received due to acoustic source S_1 at the omnidirectional microphones of an LAVS (Fig. 1) are $p_o^{S_1}(t)$, $p_h^{S_1}(t)$ and $p_v^{S_1}(t)$, and $\tau_{i,j}^{S_n}$ is the time delay of arrival of the signal (due to the source S_n) between the i-th and j-th microphones (i.e. $\tau_{h,o}^{S_1}$ is the delay between signals $p_h^{S_1}(t)$ and $p_o^{S_1}(t)$). The attenuation factor at the angular frequency ω is $\alpha(\omega)$ and κ is the speed of acoustic wave. In order to simplify the notation representation, assume

$$\chi(m_1, m_2, \xi) \triangleq [1 - \kappa \tau_{m_1,m_2}^{\xi} \alpha(\omega)]. \tag{5}$$

where m_1 and m_2 corresponds to microphone identity (m_1 or $m_2 \in [o, h, v, r, t, l]$) and ξ corresponds to acoustic source identity ($\xi \in [S_1, S_2]$). The relationship among the three received signals $p_o^{S_1}(t)$, $p_h^{S_1}(t)$, and $p_v^{S_1}(t)$ is given by

$$p_h^{S_1}(t) = \frac{p_o^{S_1}\left(t + \tau_{h,o}^{S_1}\right)}{\chi(h, o, S_1)}, \tag{6}$$

$$p_v^{S_1}(t) = \frac{p_o^{S_1}\left(t + \tau_{v,o}^{S_1}\right)}{\chi(v, o, S_1)}. \tag{7}$$

The orthogonal components of acoustic intensity due to single source S_1 are $I_x^{\mathrm{LAVS},\,S_1}$ and $I_y^{\mathrm{LAVS},\,S_1}$, and their expressions are given as

$$I_x^{\mathrm{LAVS},\,S_1} = \int_0^{\infty} \frac{\mathrm{Im}\left[\Gamma_{p_h p_o}^{S_1}(\omega)\right]}{\rho_o d\omega}\,\mathrm{d}\omega = \int_0^{\infty} \frac{\Gamma_{p_o p_o}^{S_1}(\omega)\sin\left(\omega\tau_{h,o}^{S_1}\right)}{-\rho_o d\chi(h, o, S_1)\omega}\,\mathrm{d}\omega \tag{8}$$

and

$$I_y^{\mathrm{LAVS},\,S_1} = \int_0^{\infty} \frac{Im\left[\Gamma_{p_v p_o}^{S_1}(\omega)\right]}{\rho_o d\omega}\,\mathrm{d}\omega = \int_0^{\infty} \frac{\Gamma_{p_o p_o}^{S_1}(\omega)\sin\left(\omega\tau_{v,o}^{S_1}\right)}{-\rho_o d\chi(v, o, S_1)\omega}\,\mathrm{d}\omega, \tag{9}$$

respectively. The acoustic intensity based arc-tan method will give DOA $\widehat{\theta}_{\mathrm{LAVS}}^{S_1}$ of the source S_1 and can be obtained after the substitution of expressions n Eqs (8) and (9) to Eq. (2).

Considering the TAVS (Fig. 2) where the microphones are not orthogonally arranged, there will be three microphone-pairs, so the three time-average intensity vectors are oriented along the lines joining the microphone-pairs. In such cases, projections of time-average acoustic intensity on the orthogonal axes can be used to determine the orthogonal intensity components. The projected x-axis intensity components will be averaged (not time average) to approximate x-axis intensity component and projected y-axis intensity components will be averaged (not time average) to approximate y-axis intensity component. The orthogonal components of acoustic intensity due to single source S_1 are $I_x^{\mathrm{TAVS},\,S_1}$ and $I_y^{\mathrm{TAVS},\,S_1}$, and their expressions are given as

$$\widehat{I}_x^{\mathrm{TAVS},\,S_1} = \int_0^{\infty} \frac{\Gamma_{p_l p_l}^{S_1}(\omega)\sin(\omega\tau_{k,l}^{S_1})}{6\sqrt{3}\rho_o d\chi(k, l, S_1)\omega}\,\mathrm{d}\omega + \int_0^{\infty} \frac{\Gamma_{p_l p_l}^{S_1}(\omega)\sin\left[\omega(\tau_{m,l}^{S_1} - \tau_{k,l}^{S_1})\right]}{6\sqrt{3}\rho_o d\chi(m, l, S_1)\chi(k, l, S_1)\omega}\,\mathrm{d}\omega + \int_0^{\infty} \frac{\Gamma_{p_l p_l}^{S_1}(\omega)\sin(\omega\tau_{m,l}^{S_1})}{6\sqrt{3}\rho_o d\chi(m, l, S_1)\omega}\,\mathrm{d}\omega \tag{10}$$

and

$$\widehat{I}_y^{\mathrm{TAVS},\,S_1} = \int_0^{\infty} \frac{\Gamma_{p_l p_l}^{S_1}(\omega)\sin\left[\omega(\tau_{k,l}^{S_1} - \tau_{m,l}^{S_1})\right]}{6\rho_o d\chi(k, l, S_1)\chi(m, l, S_1)\omega}\,\mathrm{d}\omega + \int_0^{\infty} \frac{\Gamma_{p_l p_l}^{S_1}(\omega)\sin(\omega\tau_{k,l}^{S_1})}{6\rho_o d\chi(k, l, S_1)\omega}\,\mathrm{d}\omega, \tag{11}$$

respectively. The arc-tan method uses these orthogonal intensity components to determine the DOA (Wajid *et al.*, 2016b).

4. DOA estimation of two coherent sources

In this section, we present a procedure for DOA estimation of acoustic sources using single AVS when two narrowband coherent sources of the different owers are present. Let initially single acoustic source S_1

is present in the field at an angle θ^{S_1} and the orthogonal intensity components are calculated using the procedure given in Sec. 3. Suppose, subsequently second source S_2 at an angular location θ^{S_2} starts emitting an acoustic signal of the same frequency as of source S_1 but of different or same power. Now two sources of the same frequency in the field are present which emit coherent acoustic signals simultaneously. When using an intensity based arc-tangent method directly, the acoustic intensity vector will not be able to estimate the direction of the second source.

Let the received signal at the three microphones of a LAVS be $p_o^{S_{12}}(t)$, $p_h^{S_{12}}(t)$, and $p_v^{S_{12}}(t)$ (as given below)

$$\begin{aligned} p_o^{S_{12}}(t) &= p_o^{S_1}(t) + p_o^{S_2}(t) \\ &= p_o^{S_1}(t) + \beta p_o^{S_1}(t), \end{aligned} \tag{12}$$

where s_{12} and s_2 in the superscript indicate the signal received due to two simultaneous sources and second source respectively, and β is the amplitude factor of the source S_2 relative to source S_1. Then

$$\begin{aligned} p_h^{S_{12}}(t) &= \frac{p_o^{S_1}\left(t+\tau_{h,o}^{S_1}\right)}{\chi(h,o,S_1)} + \frac{p_o^{S_2}\left(t+\tau_{h,o}^{S_2}\right)}{\chi(h,o,S_2)} \\ &= \frac{p_o^{S_1}\left(t+\tau_{h,o}^{S_1}\right)}{\chi(h,o,S_1)} + \frac{\beta p_o^{S_1}\left(t+\tau_{h,o}^{S_2}\right)}{\chi(h,o,S_2)} \end{aligned} \tag{13}$$

and

$$\begin{aligned} p_v^{S_{12}}(t) &= \frac{p_0^{S_1}\left(t+\tau_{v,o}^{S_1}\right)}{\chi(v,o,S_1)} + \frac{p_0^{S_2}\left(t+\tau_{v,o}^{S_2}\right)}{\chi(v,o,S_2)} \\ &= \frac{p_o^{S_1}\left(t+\tau_{v,o}^{S_1}\right)}{\chi(v,o,S_1)} + \frac{\beta p_o^{S_1}\left(t+\tau_{v,o}^{S_2}\right)}{\chi(v,o,S_2)}. \end{aligned} \tag{14}$$

The amplitude factor β is estimated as

$$\beta = \left[1 + \left(E_o^{S_{12}} - E_o^{S_1}\right)/E_o^{S_1}\right]^{1/2} - 1, \tag{15}$$

where $E_o^{S_1}$ and $E_o^{S_{12}}$ are the energies of $p_o^{S_1}(t)$ and $p_o^{S_{12}}(t)$, respectively.

The intensity spectrum components due to two sources in the field are given by

$$\begin{aligned} I_x^{\mathrm{LAVS},S_{12}} &= -\int_0^\infty \frac{\Gamma_{p_0p_0}^{S_1}(\omega)\sin\left(\omega\tau_{h,o}^{S_1}\right)}{\rho_o d\chi(h,o,S_1)\omega}\,\mathrm{d}\omega \\ &\quad -\int_0^\infty \frac{\beta\Gamma_{p_0p_0}^{S_1}(\omega)\sin\left(\omega\tau_{h,o}^{S_1}\right)}{\rho_o d\chi(h,o,S_1)\omega}\,\mathrm{d}\omega \\ &\quad -\int_0^\infty \frac{\beta\Gamma_{p_0p_0}^{S_1}(\omega)\sin\left(\omega\tau_{h,o}^{S_2}\right)}{\rho_o d\chi(h,o,S_2)\omega}\,\mathrm{d}\omega \\ &\quad -\int_0^\infty \frac{\beta^2\Gamma_{p_0p_0}^{S_1}(\omega)\sin\left(\omega\tau_{h,o}^{S_2}\right)}{\rho_o d\chi(h,o,S_2)\omega}\,\mathrm{d}\omega. \end{aligned} \tag{16}$$

Similarly,

$$\begin{aligned} I_y^{\mathrm{LAVS},S_{12}} &= -\int_0^\infty \frac{\Gamma_{p_0p_0}^{S_1}(\omega)\sin\left(\omega\tau_{v,o}^{S_1}\right)}{\rho_o d\chi(v,o,S_1)\omega}\,\mathrm{d}\omega \\ &\quad -\int_0^\infty \frac{\beta\Gamma_{p_0p_0}^{S_1}(\omega)\sin\left(\omega\tau_{v,o}^{S_1}\right)}{\rho_o d\chi(v,o,S_1)\omega}\,\mathrm{d}\omega \\ &\quad -\int_0^\infty \frac{\beta\Gamma_{p_0p_0}^{S_1}(\omega)\sin\left(\omega\tau_{v,o}^{S_2}\right)}{\rho_o d\chi(v,o,S_2)\omega}\,\mathrm{d}\omega \\ &\quad -\int_0^\infty \frac{\beta^2\Gamma_{p_0p_0}^{S_1}(\omega)\sin\left(\omega\tau_{v,o}^{S_2}\right)}{\rho_o d\chi(v,o,S_2)\omega}\,\mathrm{d}\omega. \end{aligned} \tag{17}$$

If we modify these intensity components where intensity components due to single source S_1 are removed from the intensity components due to both sources, then the resulting intensity can be used for DOA estimation of the second source in the presence of the first source. The resulting intensity components due to source S_2 are given below

$$\begin{aligned} I_x^{\mathrm{LAVS},S_{12}-S_1} &= I_x^{\mathrm{LAVS},S_{12}} - (\beta+1)I_x^{\mathrm{LAVS},S_1} \\ &= \int_0^\infty \frac{(\beta^2+\beta)\Gamma_{p_0p_0}^{S_1}(\omega)\sin\left(\omega\tau_{h,o}^{S_2}\right)}{-\rho_o d\chi(h,o,S_2)\omega}\,\mathrm{d}\omega \end{aligned} \tag{18}$$

similarly,

$$\begin{aligned} I_y^{\mathrm{LAVS},S_{12}-S_1} &= I_y^{\mathrm{LAVS},S_{12}} - (\beta+1)I_y^{\mathrm{LAVS},S_1} \\ &= \int_0^\infty \frac{(\beta^2+\beta)\Gamma_{p_0p_0}^{S_1}(\omega)\sin\left(\omega\tau_{v,o}^{S_2}\right)}{-\rho_o d\chi(v,o,S_2)\omega}\,\mathrm{d}\omega, \end{aligned} \tag{19}$$

therefore, DOA $\widehat{\theta}_{\mathrm{LAVS}}^{S_2}$ of the second source using LAVS can be obtained after the substitution of expressions in Eqs (18) and (19) to Eq. (2). If yet third source of same frequency begins to emit, then the same technique can be extended for finding DOA of an additional source in the field.

The above concept has been applied to TAVS configuration also. For the two source case, let the received signal at the three microphones are $p_k^{S_{12}}(t)$, $p_l^{S_{12}}(t)$, and $p_m^{S_{12}}(t)$ (as given below)

$$\begin{aligned} p_l^{S_{12}}(t) &= p_l^{S_1}(t) + p_l^{S_2}(t) \\ &= p_l^{S_1}(t) + \beta p_l^{S_1}(t), \end{aligned} \tag{20}$$

$$\begin{aligned} p_m^{S_{12}}(t) &= \frac{p_l^{S_1}\left(t+\tau_{m,l}^{S_1}\right)}{\chi(m,l,S_1)} + \frac{p_l^{S_2}\left(t+\tau_{m,l}^{S_2}\right)}{\chi(m,l,S_2)} \\ &= \frac{p_l^{S_1}\left(t+\tau_{m,l}^{S_1}\right)}{\chi(m,l,S_1)} + \frac{\beta p_l^{S_1}\left(t+\tau_{m,l}^{S_2}\right)}{\chi(m,l,S_2)}, \end{aligned} \tag{21}$$

and

$$p_k^{S_{12}}(t) = \frac{p_l^{S_1}\left(t+\tau_{k,l}^{S_1}\right)}{\chi(k,l,S_1)} + \frac{p_l^{S_2}\left(t+\tau_{k,l}^{S_2}\right)}{\chi(k,l,S_2)}$$
$$= \frac{p_l^{S_1}\left(t+\tau_{k,l}^{S_1}\right)}{\chi(k,l,S_1)} + \frac{\beta p_l^{S_1}\left(t+\tau_{k,l}^{S_2}\right)}{\chi(k,l,S_2)}. \quad (22)$$

The intensity spectrum components due to two sources in the field are given by

$$I_y^{\mathrm{TAVS},S_{12}} = \int_0^\infty \frac{\Gamma_{p_lp_l}^{S_1}(\omega)\sin[\omega(\tau_{m,l}^{S_1}-\tau_{k,l}^{S_1})]}{6\rho_o d\chi(k,l,S_1)\chi(m,l,S_1)\omega}\,\mathrm{d}\omega$$
$$+\int_0^\infty \frac{\beta\Gamma_{p_lp_l}^{S_1}(\omega)\sin[\omega(\tau_{m,l}^{S_2}-\tau_{k,l}^{S_1})]}{6\rho_o d\chi(k,l,S_1)\chi(m,l,S_2)\omega}\,\mathrm{d}\omega$$
$$+\int_0^\infty \frac{\beta\Gamma_{p_lp_l}^{S_1}(\omega)\sin[\omega(\tau_{m,l}^{S_1}-\tau_{k,l}^{S_2})]}{6\rho_o d\chi(k,l,S_2)\chi(m,l,S_1)\omega}\,\mathrm{d}\omega$$
$$+\int_0^\infty \frac{\beta^2\Gamma_{p_lp_l}^{S_1}(\omega)\sin[\omega(\tau_{m,l}^{S_2}-\tau_{k,l}^{S_2})]}{6\rho_o d\chi(k,l,S_2)\chi(m,l,S_2)\omega}\,\mathrm{d}\omega$$
$$-\int_0^\infty \frac{(1+\beta)\Gamma_{p_lp_l}^{S_1}(\omega)\sin(\omega\tau_{m,l}^{S_1})}{6\rho_o d\chi(m,l,S_1)\omega}\,\mathrm{d}\omega$$
$$-\int_0^\infty \frac{\beta(1+\beta)\Gamma_{p_lp_l}^{S_1}(\omega)\sin(\omega\tau_{m,l}^{S_2})}{6\rho_o d\chi(m,l,S_2)\omega}\,\mathrm{d}\omega \quad (23)$$

and

$$I_x^{\mathrm{TAVS},S_{12}} = -\frac{(1+\beta)}{3\sqrt{3}\rho_o d}\int_0^\infty \frac{\Gamma_{p_lp_l}^{S_1}(\omega)\sin(\omega\tau_{m,l}^{S_1})}{\chi(m,l,S_1)\omega}\,\mathrm{d}\omega$$
$$-\frac{\beta}{3\sqrt{3}\rho_o d}\int_0^\infty \frac{\Gamma_{p_lp_l}^{S_1}(\omega)\sin(\omega\tau_{m,l}^{S_2})}{\chi(m,l,S_2)\omega}\,\mathrm{d}\omega$$
$$+\frac{1}{6\sqrt{3}\rho_o d}\int_0^\infty \frac{\Gamma_{p_lp_l}^{S_1}(\omega)\sin(\omega\tau_{t,l}^{S_1}-\omega\tau_{m,l}^{S_1})}{\chi(t,l,S_1)\chi(m,l,S_1)\omega}\,\mathrm{d}\omega$$
$$+\frac{\beta}{6\sqrt{3}\rho_o d}\int_0^\infty \frac{\Gamma_{p_lp_l}^{S_1}(\omega)\sin(\omega\tau_{t,l}^{S_2}-\omega\tau_{m,l}^{S_1})}{\chi(t,l,S_2)\chi(m,l,S_1)\omega}\,\mathrm{d}\omega$$
$$+\frac{\beta}{6\sqrt{3}\rho_o d}\int_0^\infty \frac{\Gamma_{p_lp_l}^{S_1}(\omega)\sin(\omega\tau_{t,l}^{S_1}-\omega\tau_{m,l}^{S_2})}{\chi(t,l,S_1)\chi(m,l,S_2)\omega}\,\mathrm{d}\omega$$
$$+\frac{\beta^2}{6\sqrt{3}\rho_o d}\int_0^\infty \frac{\Gamma_{p_lp_l}^{S_1}(\omega)\sin(\omega\tau_{t,l}^{S_2}-\omega\tau_{m,l}^{S_2})}{\chi(t,l,S_2)\chi(m,l,S_2)\omega}\,\mathrm{d}\omega$$
$$-\frac{(1+\beta)}{6\sqrt{3}\rho_o d}\int_0^\infty \frac{\Gamma_{p_lp_l}^{S_1}(\omega)\sin(\omega\tau_{t,l}^{S_1})}{\chi(t,l,S_1)\omega}\,\mathrm{d}\omega$$
$$-\frac{\beta(1+\beta)}{6\sqrt{3}\rho_o d}\int_0^\infty \frac{\Gamma_{p_lp_l}^{S_1}(\omega)\sin(\omega\tau_{t,l}^{S_2})}{\chi(t,l,S_2)\omega}\,\mathrm{d}\omega. \quad (24)$$

The resulting intensity components due to source S_2 are given below

$$I_x^{\mathrm{TAVS},S_{12}-S_1} = I_x^{\mathrm{TAVS},S_{12}} - (\beta+1)I_x^{\mathrm{TAVS},S_1}$$
$$\simeq -\frac{(\beta^2+\beta)}{3\sqrt{3}\rho_o d}\int_0^\infty \frac{\Gamma_{p_lp_l}^{S_1}(\omega)\sin(\omega\tau_{m,l}^{S_2})}{\chi(m,l,S_2)\omega}\,\mathrm{d}\omega$$
$$+\frac{(\beta^2+\beta)}{6\sqrt{3}\rho_o d}\int_0^\infty \frac{\Gamma_{p_lp_l}^{S_1}(\omega)\sin(\omega\tau_{k,l}^{S_2}-\omega\tau_{m,l}^{S_2})}{\chi(k,l,S_2)\chi(m,l,S_2)\omega}\,\mathrm{d}\omega$$
$$-\frac{(\beta^2+\beta)}{6\sqrt{3}\rho_o d}\int_0^\infty \frac{\Gamma_{p_lp_l}^{S_1}(\omega)\sin(\omega\tau_{k,l}^{S_2})}{\chi(k,l,S_2)\omega}\,\mathrm{d}\omega \quad (25)$$

and

$$I_y^{\mathrm{TAVS},S_{12}-S_1} = I_y^{\mathrm{TAVS},S_{12}} - (\beta+1)I_y^{\mathrm{TAVS},S_1}$$
$$\simeq -\frac{(\beta^2+\beta)}{6\sqrt{3}\rho_o d}\int_0^\infty \frac{\Gamma_{p_lp_l}^{S_1}(\omega)\sin(\omega\tau_{m,l}^{S_2})}{\chi(m,l,S_2)\omega}\,\mathrm{d}\omega$$
$$+\frac{(\beta^2+\beta)}{6\sqrt{3}\rho_o d}\int_0^\infty \frac{\Gamma_{p_lp_l}^{S_1}(\omega)\sin\{\omega(\tau_{m,l}^{S_2}-\tau_{k,l}^{S_2})\}}{\chi(k,l,S_2)\chi(m,l,S_2)\omega}\,\mathrm{d}\omega, \quad (26)$$

therefore, DOA $\widehat{\theta}_{\mathrm{TAVS}}^{S_2}$ of the second source S_2 using TAVS can be obtained after the substitution of expressions in Eqs (25) and (26) to Eq. (2).

We have used TAVS and LAVS configurations, however, the presented technique may be extended to any AVS configurations.

5. Simulation setup and results

The experimental environment has been generated using the Finite-Element Method (FEM) tool viz. COMSOL, where two coherent omnidirectional point source signals (25 ms duration) are generated and recorded by omnidirectional microphones of an AVS (LAVS or TAVS) with a sampling rate of 48 kHz. The acoustic sources generate sinusoidal signals of frequency 1 kHz and are kept at a distance of 1 m from the AVS device, and microphone separation d is 10 mm. The simulation is repeated for the different angular locations of the sources and with different values of SNR.

The white Gaussian noise has been added to all the three signals acquired by the microphones of an AVS configuration. The DOA estimation performance in the presence of additive white Gaussian noise (AWGN) is represented in terms of *root mean square angular error* (RMSAE), which is defined as

$$\mathrm{RMSAE} = \sqrt{\frac{\sum_{i=1}^{N}\left\{\widehat{\theta}_i-\theta\right\}^2}{N}}, \quad (27)$$

where θ is the true DOA of the acoustic source, $\widehat{\theta_i}$ is its estimate at the i-th realization of the noisy AVS signals, and N (N = 10000) is the total number of independent realizations considering AWGN (ranging from 10 dB to 30 dB) at every microphone. All results are calculated after the removal of 5% outliers from each end of the probability distribution of DOA estimate.

The results for DOA estimation when second coherent acoustic source enters in the field in the presence of first acoustic source are given in Tables 1 and 2 for LAVS and TAVS respectively.

In these tables, six cases have been considered with different angular locations of the first source S_1 and second source S_2. In each case, the angular separation between the two sources is 5°. The RMSAE in degrees has been calculated for the estimated DOA of S_2 for SNR value from 10 dB to 30 dB with an increment of 4 dB and for no noise case. It is observed that even for very small angular separation i.e. 5° and at SNR of 30 dB, the RMSAE of the estimated DOA of S_2 is of order 0.5° and 0.4° for LAVS and TAVS respectively. The maximum RMSAE for the source S_2 is 3.808° at 10 dB for the TAVS. The results of LAVS is better for the no noise case, however, when noise is present TAVS outperforms the LAVS in terms of RMSAE Also, it is observed that with the decrease in SNR, the rate of increase in RMSAE is more for LAVS than the TAVS. So in this paper, we will use the TAVS configuration for further analysis on the tracking of coherent sources.

We have also studied continuous tracking of two sequential coherent sources using a single AVS. Consider a scenario where source S_1 is changing its angular position in the presence of a coherent stationary interfering source INT_1. Assuming that source S_1 was present at 60° in the field at time $t = T$, then at time $t = 2T$ an interfering source (INT_1) starts emitting a coherent signal at an angle 55° followed by source S_1 continuously changing its location (after every time interval of T) from 60° to 75° with an increment of 5°. The moving source description in the presence of interfering source and acoustic intensity estimation at different time instances is also depicted in Fig. 3. The results for this scenario with $\beta = 3/2$ at different time instances are given in Table 3, for fixed value of SNR, it is observed that RMSAE of DOA estimate of S_1 or INT_1 increases with time up to $3T$, which is due to the addition of bias in intensity estimate and cumulative noise in the intensity estimate.

Consider the scenario where source S_1 and source S_2 are changing their angular positions alternatively, with the assumption that one source is stationary while the other source is changing its location. Based on this assumption we have tracked the angular locations of two sources. This situation may arise when decoy also changes its location to deceive surveillance devices. Assuming that S_1 was at 60° at time $t = T$ then S_2 starts emitting coherent signal at location 65°, then S_2 does not change its location while S_1 moves to 55°. Thereafter, S_2 moves to 70° and then S_1 moves to 55°. The description of two moving sources changing their angular position alternatively at different time instances is also depicted in Fig. 4, it also

Table 1. RMSAE [°] of second coherent sources S_2 using a single LAVS in the presence of first source S_1 with $\beta = 3/2$ (note: S_1 and S_2 are two coherent sources emitting sinusoidal of 1 kHz).

	True DOA of		RMSAE [°] of estimated DOA of source S_2						
	S_1	S_2	infinity	30 dB	26 dB	22 dB	18 dB	14 dB	10 dB
Case 1	5°	10°	0.020	0.553	0.780	1.333	2.118	3.580	5.931
Case 2	35°	40°	0.004	0.436	0.639	1.081	1.733	2.733	4.428
Case 3	40°	45°	0.000	0.428	0.624	1.064	1.721	2.750	4.507
Case 4	40°	50°	0.003	0.438	0.652	1.093	1.753	2.779	4.530
Case 5	75°	80°	0.014	0.559	0.831	1.406	2.262	3.672	6.022
Case 6	90°	85°	0.010	0.584	0.875	1.490	2.400	3.890	6.410

Table 2. RMSAE [°] of second coherent sources S_2 using a single TAVS in the presence of first source S_1 with $\beta = 3/2$ (note: S_1 and S_2 are two coherent sources emitting sinusoidal of 1 kHz).

	True DOA of		RMSAE [°] of estimated DOA of source S_2						
	S_1	S_2	infinity	30 dB	26 dB	22 dB	18 dB	14 dB	10 dB
Case 1	5°	10°	0.136	0.381	0.402	0.742	1.256	2.099	3.551
Case 2	35°	40°	0.239	0.419	0.341	0.674	1.207	2.043	3.369
Case 3	40°	45°	0.205	0.411	0.365	0.688	1.225	2.055	3.364
Case 4	40°	50°	0.149	0.386	0.401	0.745	1.261	2.116	3.494
Case 5	75°	80°	0.249	0.428	0.737	1.101	1.637	2.444	3.732
Case 6	90°	85°	0.273	0.449	0.758	1.127	1.646	2.466	3.808

Time	$t = T$	$t = 2T$	$t = 3T$	$t = 4T$	$t = 5T$
Event	Only S_1 is emitting signal at 60°	INT_1 starts emitting signal at 55° in the presence of S_1 (at 60°)	S_1 changed its location to 65° in the presence of INT_1 (at 55°)	S_1 changed its location to 70° in the presence of INT_1 (at 55°)	S_1 changed its location to 75° in the presence of INT_1 (at 55°)
Action	Calculate the acoustic intensity components ($I_x^{S_1,T}$and $I_y^{S_1,T}$) due to S_1 using Eqs (10) and (11) then calculate the DOA of S_1 using Eq. (2).	Calculate the acoustic intensity components due to both sources S_1 and INT_1 using Eqs (23) and (24). The intensity ($I_x^{\mathrm{INT}_1,2T}$ and $I_y^{\mathrm{INT}_1,2T}$) due to single source INT_1 in the presence of S_1 can be estimated using Eq. (25) and (26), thereby DOA of INT_1.	For all the time instances, calculate the acoustic intensity components due to both sources S_1 and INT_1 using Eqs (23) and (24). The intensity components ($I_x^{S_1,t}$and $I_y^{S_1,t}$) at time t due to a single source S_1 in the presence of INT_1 can be estimated by employing $I_x^{\mathrm{INT}_1,2T}$ and $I_y^{\mathrm{INT}_1,2T}$ in Eqs (25) and (26), thereby, DOA of S_1 at all the time instances.		

Fig. 3. Description of moving sources with time instances, source S_1 is moving in the presence of interfering source INT_1. Action row shows the procedure for calculating acoustic intensities and DOA.

Table 3. RMSAE (Degrees) for a moving sources S_1 in the presence of stationary interfering coherent source INT_1 for TAVS, with $\beta = 3/2$. Location of interfering source is fixed at 55°.

Source	True DOA (time)	RMSAE [°] of estimated DOA						
		infinity	30 dB	26 dB	22 dB	18 dB	14 dB	10 dB
S_1	60° ($t = T$)	0.005	0.201	0.316	0.453	0.802	1.156	1.958
INT_1	55° ($t = 2T$)	0.084	0.366	0.567	0.758	1.423	1.981	3.423
S_1	65° ($t = 3T$)	0.070	0.728	1.152	1.841	2.890	4.627	7.368
S_1	70° ($t = 4T$)	0.149	0.744	1.145	1.835	2.894	4.620	7.406
S_1	75° ($t = 5T$)	0.187	0.741	1.158	1.852	2.935	4.531	7.398

Time	$t = T$	$t = 2T$	$t = 3T$	$t = 4T$	$t = 5T$
Event	Only S_1 is emitting signal at 60°	S_2 starts emitting signal at 65° in the presence of S_1 (at 60°)	S_1 changed its location to 55° in the presence of S_2 (at 65°)	S_2 changed its location to 70° in the presence of S_1 (at 55°)	S_1 changed its location to 50° in the presence of S_2 (at 70°)
Action	Calculate the acoustic intensity components ($I_x^{S_1,T}$ and $I_y^{S_1,T}$) due to S_1 using Eqs (10) and (11) then calculate the DOA of S_1 using Eq. (2).	Calculate the acoustic intensity components ($I_x^{S_{12},2T}$ and $I_y^{S_{12},2T}$) due to both sources S_1 and S_2 using Eqs (23) and (24). The intensity components ($I_x^{S_{12},2T}$ and $I_y^{S_{12},2T}$) due to a single source S_2 in the presence of S_1 can be estimated by employing Eqs (25) and (26), thereby DOA of S_2.	Calculate the acoustic intensity components ($I_x^{S_{21},3T}$ and $I_y^{S_{21},3T}$) due to both sources S_1 and S_2 using Eqs (23) and (24). The intensity components ($I_x^{S_1,3T}$ and $I_y^{S_1,3T}$) due to a single source S_1 in the presence of S_2 can be estimated by employing ($I_x^{S_2,2T}$ and $I_y^{S_2,2T}$) Eqs (25) and (26), thereby DOA of S_1.	Calculate the acoustic intensity components ($I_x^{S_{12},4T}$and $I_y^{S_{12},4T}$) due to both sources S_1 and S_2 using Eqs (23) and (24). The intensity components ($I_x^{S_2,4T}$ and $I_y^{S_2,4T}$) due to a single source S_1 in the presence of S_2 can be estimated by employing ($I_x^{S_1,3T}$ and $I_y^{S_1,3T}$) Eqs (25) and (26), thereby DOA of S_2.	Calculate the acoustic intensity components ($I_x^{S_{21},5T}$ and $I_y^{S_{21},5T}$) due to both sources S_1 and S_2 using Eqs (23) and (24). The intensity components ($I_x^{S_1,5T}$ and $I_y^{S_1,5T}$) due to a single source S_1 in the presence of S_2 can be estimated by employing ($I_x^{S_2,4T}$ and $I_y^{S_2,4T}$) Eqs (25) and (26), thereby DOA of S_1.

Fig. 4. Description of moving sources with time instances, source S_1 and source S_2 are changing their angular positions alternatively. Action row shows the procedure for calculating acoustic intensities and DOA.

shows the procedure for calculating acoustic intensity at those time instances, thereby, tracking the angular location of the sources. We have estimated the DOA of both sources in such scenario. The results for this scenario for different time instances and for different energy of the sources are given in Tables 4–6.

Table 4. RMSAE [°] for two sequential coherent sources for TAVS with $\beta = 1$ (energy of S_2 is equal to energy of S_1).

Source	True DOA (time)	RMSAE [°] of estimated DOA						
		infinity	30 dB	26 dB	22 dB	18 dB	14 dB	10 dB
S_1	60° ($t = T$)	0.005	0.198	0.318	0.502	0.800	1.263	2.007
S_2	65° ($t = 2T$)	0.070	0.447	0.699	1.119	1.764	2.793	4.494
S_1	55° ($t = 3T$)	0.083	0.599	0.951	1.500	2.354	3.742	5.998
S_2	70° ($t = 4T$)	0.150	0.729	1.137	1.779	2.852	4.590	7.321
S_1	50° ($t = 5T$)	0.148	0.832	1.313	2.052	3.298	5.206	8.336

Table 5. RMSAE [°] for two sequential coherent sources for TAVS with $\beta = 2/3$ (energy of S_2 is β^2 times than the energy of S_1).

Source	True DOA (time)	RMSAE [°] of estimated DOA						
		infinity	30 dB	26 dB	22 dB	18 dB	14 dB	10 dB
S_1	60° ($t = T$)	0.005	0.200	0.315	0.505	0.797	1.269	2.037
S_2	65° ($t = 2T$)	0.070	0.585	0.911	1.434	2.313	3.704	5.886
S_1	55° ($t = 3T$)	0.083	0.512	0.802	1.278	2.053	3.262	5.143
S_2	70° ($t = 4T$)	0.150	0.923	1.441	2.268	3.685	5.841	9.194
S_1	50° ($t = 5T$)	0.148	0.709	1.089	1.727	2.757	4.432	6.9744

Table 6. RMSAE [°] for two sequential coherent sources for TAVS with $\beta = 3/2$ (energy of S_2 is β^2 times than the energy of S_1).

Source	True DOA (time)	RMSAE [°] of estimated DOA						
		infinity	30 dB	26 dB	22 dB	18 dB	14 dB	10 dB
S_1	60° ($t = T$)	0.005	0.201	0.317	0.506	0.796	1.273	2.006
S_2	65° ($t = 2T$)	0.070	0.359	0.568	0.891	1.417	2.243	3.570
S_1	55° ($t = 3T$)	0.083	0.728	1.163	1.815	2.903	4.618	7.310
S_2	70° ($t = 4T$)	0.150	0.599	0.942	1.470	2.332	3.373	5.926
S_1	50° ($t = 5T$)	0.148	1.006	1.592	2.503	3.991	6.356	10.224

Table 4 show the RMSAE results of the sources S_1 and S_2 when the energy of S_2 is equal to the energy of S_1 ($\beta = 1$). It is observed that when noise is present, the RMSAE increases continuously for every alternate position estimate of the two sources with equal energy, this is due to the cumulative effect of noise on the estimate of modified intensity, thereby, deteriorate the DOA estimate. Table 5 show the RMSAE results of the sources S_1 and S_2 when the energy of S_2 is 0.444 times than the energy of S_1 ($\beta = 2/3$). It has been observed that an increase in RMSAE with the progressive change in alternating positions of the sources is less for the source having higher energy. For example, the RMSAE is decreased at $t = 3T$ ($t = 5T$) than at $t = 2T$ ($t = 4T$) because the effect of cumulative noise is less on the DOA estimate of source S_1 due to its higher energy compared to the source S_2. Table 6 show the RMSAE results of the sources S_1 and S_2 when the energy of S_2 is 2.25 times than the energy of S_1 ($\beta = 3/2$). The energy of source S_2 is higher than the source S_1. Therefore, the progressive change in alternating positions of the sources causes decreased in RMSAE at $t = 4T$ than at $t = 3T$. For the no noise case as given in Tables 4–6, the RMSAE is increasing slightly with the alternating positions of the sources, this is due to the addition of bias in the estimate on every alternate position estimation. This bias does not vary with the relative change in the energies of the two sources.

6. Conclusions

A new approach has been presented for the localization of multiple coherent sources using a single AVS. For two different AVS configurations, an expression has been derived for the DOA estimation in the presence of coherent sources using signals acquired by single AVS. It has been shown that the DOA of two coherent sources can be estimated using any AVS configuration (LAVS or TAVS) consisting of Omni-directional microphones only. The main advantage of these estimators is that they can provide instantaneous DOA estimates of multiple coherent sources. The performance of the proposed algorithm has been presented in

terms of RMSAE for stationary and moving coherent sources. Further research will include the development of a range estimation algorithm, performance analysis in the reverberant environment, practical issues and implementation.

References

1. Cao J., Liu J., Wang J., Lai, X. (2016), Acoustic vector sensor: reviews and future perspectives, *IET Signal Processing*, **11**(1): 1–9, doi: 10.1049/iet-spr.2016.0111.
2. Chen H., Zhao J. (2005), Coherent signal-subspace processing of acoustic vector sensor array for DOA estimation of wideband sources, *Signal Processing*, **85**(4): 837–847, doi: 10.1016/j.sigpro.2004.07.030.
3. Chung J. (1978), Cross-spectral method of measuring acoustic intensity without error caused by instrument phase mismatch, *The Journal of the Acoustical Society of America*, **64**(6): 1613–1616, doi: 10.1121/1.382145.
4. de Bree H.-E. (2003), An overview of microflown technologies, *Acta Acustica united with Acustica*, **89**(1): 163–172.
5. Dmochowski J., Benesty J., Affes S. (2007), Direction of arrival estimation using the parameterized spatial correlation matrix, *IEEE Transactions on Audio, Speech, and Language Processing*, **15**(4): 1327–1339, doi: 10.1109/TASL.2006.889795.
6. Du W., Kirlin R.L. (1991), Improved spatial smoothing techniques for DOA estimation of coherent signals, *IEEE Transactions on Signal Processing*, **39**(5): 1208–1210, doi: 10.1109/78.80975.
7. Evans J.E., Johnson J.R., Sun D. (1982), *Application of advanced signal processing techniques to angle of arrival estimation in ATC navigation and surveillance systems*, Technical Report, Lincoln Laboratory.
8. Fahy F.J. (1977), Measurement of acoustic intensity using the cross-spectral density of two microphone signals, *The Journal of the Acoustical Society of America*, **62**(4): 1057–1059, doi: 10.1121/1.381601.
9. Han F.-M., Zhang S.-H. (2004), Separation of coherent multi-path signals with improved MUSIC algorithm, *Systems Engineering and Electronics*, **26**(6): 721–723, 763.
10. Han F.-M., Zhang X.-D. (2005), An ESPRIT-like algorithm for coherent DOA estimation, *IEEE Antennas and Wireless Propagation Letters*, **4**: 443–446, doi: 10.1109/LAWP.2005.860194.
11. Hawkes M., Nehorai A. (1998), Acoustic vector-sensor beamforming and Capon direction estimation, *IEEE Transactions on Signal Processing*, **46**(9): 2291–2304, doi: 10.1109/ICASSP.1995.479926.
12. Hochwald B., Nehorai A. (1996), Identifiability in array processing models with vector-sensor applications, *IEEE Transactions on Signal Processing*, **44**(1): 83–95, doi: 10.1109/78.482014.
13. Kotus J. (2012), Multiple sound sources localization in real time using acoustic vector sensor, [in:] Dziech A., Czyżewski A. [Eds], *Multimedia Communications, Services and Security. MCSS 2012. Communications in Computer and Information Science*, Vol. 287, pp. 168–179, Springer, Berlin, Heidelberg, doi: 10.1007/978-3-642-30721-8_17.
14. Kotus J. (2015), Multiple sound sources localization in free field using acoustic vector sensor, *Multimedia tools and applications*, **74**(12): 4235–4251, doi: 10.1007/s11042-013-1549-y.
15. Kotus J., Czyżewski A. (2010), Acoustic radar employing particle velocity sensors, [in:] Nguyen N.T., Zgrzywa A., Czyżewski A. [Eds], *Advances in Multimedia and Network Information System Technologies. Advances in Intelligent and Soft Computing*, vol 80, pp. 93–103, Springer, Berlin, Heidelberg, doi: 10.1007/978-3-642-14989-4_9.
16. Kotus J., Czyżewski A., Kostek B. (2016), 3D acoustic field intensity probe design and measurements, *Archives of Acoustics*, **41**(4): 701–711, doi: 10.1515/aoa-2016-0067.
17. Kotus J., Kostek B. (2015), Measurements and visualization of sound intensity around the human head in free field using acoustic vector sensor, *Journal of the Audio Engineering Society*, **63**(1/2): 99–109, doi: 10.17743/jaes.2015.0009.
18. Kotus J., Lopatka K., Czyżewski A. (2014), Detection and localization of selected acoustic events in acoustic field for smart surveillance applications, *Multimedia Tools and Applications*, **68**(1): 5–21, doi: 10.1007/s11042-012-1183-0.
19. Krishnappa G. (1981), Cross-spectral method of measuring acoustic intensity by correcting phase and gain mismatch errors by microphone calibration, *The Journal of the Acoustical Society of America*, **69**(1): 307–310, doi: 10.1121/1.385314.
20. Liu Z., Ruan X., He J. (2013), Efficient 2-D DOA estimation for coherent sources with a sparse acoustic vector-sensor array, *Multidimensional Systems and Signal Processing*, **24**(1): 105–120, doi: 10.1007/s11045-011-0158-z.
21. Lockwood M.E., Jones D.L. (2006), Beamformer performance with acoustic vector sensors in air, *The Journal of the Acoustical Society of America*, **119**(1): 608–619, doi: 10.1121/1.2139073.
22. Miah K.H., Hixon E.L. (2010), Design and performance evaluation of a broadband three dimensional acoustic intensity measuring system, *The Journal of the Acoustical Society of America*, **127**(4): 2338–2346, doi: 10.1121/1.3327508.
23. Moschioni G., Saggin B., Tarabini M. (2007), Sound source identification using coherence- and intensity-based methods, *Instrumentation and Measurement, IEEE Transactions on*, **56**(6): 2478–2485, doi: 10.1109/TIM.2007.908246.
24. Nehorai A., Paldi E. (1994), Acoustic vector-sensor array processing, *Signal Processing, IEEE Transactions on*, **42**(9): 2481–2491, doi: 10.1109/78.317869.

25. Odya P., Kotus J., Szczodrak M., Kostek B. (2017), Sound intensity distribution around organ pipe, *Archives of Acoustics*, **42**(1): 13–22, doi: 10.1515/aoa-2017-0002.

26. Palanisamy P., Kalyanasundaram N., Swetha P. (2012), Two-dimensional DOA estimation of coherent signals using acoustic vector sensor array, *Signal Processing*, **92**(1): 19–28, doi: 10.1016/j.sigpro.2011.05.021.

27. Pillai S.U., Kwon, B.H. (1989), Forward/backward spatial smoothing techniques for coherent signal identification, *IEEE Transactions on Acoustics, Speech, and Signal Processing*, **37**(1): 8–15, doi: 10.1109/29.17496.

28. Qian C., Huang L., Zeng W.-J., So H.C. (2014), Direction-of-arrival estimation for coherent signals without knowledge of source number, *IEEE Sensors Journal* **14**(9): 3267–3273, doi: 10.1109/JSEN.2014.2327633.

29. Rinford J. (1981), Technical review to advance techniques in acoustical, *Electrical and Mechanical Measurements*, Bruel and Kjær, DK-2850 NAERUM, Denmark, **2**: 3.

30. Shan T.-J., Wax M., Kailath T. (1985), On spatial smoothing for direction-of-arrival estimation of coherent signals, *IEEE Transactions on Acoustics, Speech, and Signal Processing*, **33**(4): 806–811, doi: 10.1109/TASSP.1985.1164649.

31. Thompson J., Tree D. (1981), Finite difference approximation errors in acoustic intensity measurements, *Journal of Sound and Vibration*, **75**(2): 229–238, doi: 10.1016/0022-460X(81)90341-2.

32. Wajid M., Kumar A., Bahl R. (2016a), Bearing estimation in a noisy and reverberant environment using an air acoustic vector sensor, *IUP Journal of Electrical and Electronics Engineering*, **9**(2): 53.

33. Wajid M., Kumar A., Bahl R. (2016b), Design and analysis of air acoustic vector-sensor configurations for two-dimensional geometry, *The Journal of the Acoustical Society of America*, **139**(5): 2815–2832, doi: 10.1121/1.4948566.

34. Wajid M., Kumar A., Bahl R. (2017a), Direction-finding accuracy of an air acoustic vector sensor in correlated noise field, *2017 4th International Conference on Signal Processing, Computing and Control (ISPCC)*, IEEE, pp. 21–25, doi: 10.1109/ISPCC.2017.8269643.

35. Wajid M., Kumar A., Bahl R. (2017b), Direction-of-arrival estimation algorithms using single acoustic vector-sensor, *2017 International Conference on Multimedia, Signal Processing and Communication Technologies (IMPACT)*, IEEE, pp. 84–88, doi: 10.1109/MSPCT.2017.8363979.

36. Wajid M., Kumar A., Bahl R. (2017c), Direction-of-arrival estimation algorithms using single acoustic vector-sensor, *2017 International Conference on Multimedia, Signal Processing and Communication Technologies (IMPACT)*, IEEE, pp. 84–88, doi: 10.1109/MSPCT.2017.8363979.

37. Wang H., Kaveh M. (1985), Coherent signal-subspace processing for the detection and estimation of angles of arrival of multiple wide-band sources, *IEEE Transactions on Acoustics, Speech, and Signal Processing*, **33**(4): 823–831, doi: 10.1109/TASSP.1985.1164667.

38. Wu Y., Li G., Hu Z., Hu Y. (2014), Unambiguous directions of arrival estimation of coherent sources using acoustic vector sensor linear arrays, *IET Radar, Sonar & Navigation*, **9**(3): 318–323, doi: 10.1049/iet-rsn.2014.0191.